Temperature-dependent phonon spectrum of transition metal dichalcogenides calculated from the spectral energy density: Lattice thermal conductivity as an application

Arash Mobaraki, Cem Sevik, Haluk Yapicioglu, Deniz Çakır, and Oğuz Gülseren

Phys. Rev. B **100**, 035402 — Published 2 July 2019

DOI: 10.1103/PhysRevB.100.035402

Temperature Dependent Phonon Spectrum of Transition Metal Dichalcogenides Calculated from Spectral Energy Density: Lattice Thermal Conductivity as an Application

Arash Mobaraki,[1] Cem Sevik,[2] Haluk Yapicioglu,[3] Deniz Çakır,[4] and Oğuz Gülseren[1]

[1] *Department of Physics, Bilkent University, Ankara 06800, Turkey*
[2] *Department of Mechanical Engineering, Faculty of Engineering, Eskisehir Technical University, Eskisehir, TR 26555, Turkey.*
[3] *Department of Industrial Engineering, Faculty of Engineering, Eskisehir Technical University, Eskisehir, TR 26555, Turkey.*
[4] *Department of Physics and Astrophysics, University of North Dakota, Grand Forks, North Dakota 58202, USA.*

Predicting the mechanical and thermal properties of quasi two dimensional transition metal dichalcogenides (TMDs) is an essential task necessary for their implementation in device applications. Although, rigorous density functional theory based calculations are able to predict mechanical and electronic properties, mostly they are limited to zero temperature. Classical molecular dynamics facilitates the investigation of temperature dependent properties, but its performance highly depends on the potential used for defining interactions between the atoms. In this study, we calculated temperature dependent phonon properties of single layer TMDs, namely MoS_2, $MoSe_2$, WS_2, and WSe_2, by utilizing Stillinger-Weber type potentials with optimized sets of parameters with respect to the first-principles results. The phonon lifetimes and contribution of each phonon mode in thermal conductivities in these monolayer crystals are systematically investigated by means of spectral energy density method based on molecular dynamics simulations. The obtained results from this approach are in good agreement with previously available results from Green-Kubo method. Moreover, detailed analysis of lattice thermal conductivity, including temperature dependent mode decomposition through the entire Brillouin zone, brought more light on thermal properties of these 2D crystals. The LA and TA acoustic branches contribute most to the lattice thermal conductivity, while ZA mode contribution is less because of the quadratic dispersion around Brillouin zone center, in particular in $MoSe_2$ due to the phonon anharmonicity, evident from the red shift, especially in optical modes, by increasing temperature. For all the considered 2D crystals, the phonon lifetime values are compelled by transition metal atoms, whereas the group velocity spectrum is dictated by chalcogen atoms. Overall, the lattice thermal conductivity is linearly proportional with inverse temperature.

I. INTRODUCTION

A new era of nano-device engineering has been started after fabricating isolated single layer of graphite named as graphene. Although this carbon allotrope has many extraordinary properties, its zero band gap, which imposes a challenge for possible band gap engineering, is the main setback of it for device applications. Hexagonal Boron Nitride (h-BN) is another planar two dimensional (2D) material, contrary to the graphene it has an intrinsic band gap, however being an insulator restricts its applications especially for electronics. On the other hand, a new class of semiconductor 2D materials, known as Transition Metal Dichalcogenides (TMDs), MX_2 (where M stands for transition metal atom, and X = S, Se, Te) are both theoretically and experimentally proven to be promising candidate for wide range applications where graphene and h-BN are inadequate[1–4]. For instance, they possess indirect to direct band-gap transition with number of layers[5], and semiconductor to metal transition induced by overlaying substrates[6]. Also, they exhibit distinctive optical properties, chemically versatility[7] and tunable spin and valley degrees of freedoms[8]. These outstanding properties make them ideal candidates in particular for flexible electronic and optoelectronic devices[9–14], and thermoelectric applications[15–19].

Since thermal and mechanical properties of materials are crucial in any device applications, many experimental and theoretical investigations have been carried out in order to determine temperature dependent properties of single layer TMDs[20]. First-principles calculations[21,22] estimated positive thermal expansion coefficient at low temperature for most common TMDs, which are WS_2, WSe_2, MoS_2 and $MoSe_2$, while it was reported to be negative for graphene[23]. Besides, they have much smaller thermal conductivities compared to graphene and h-BN. For instance, thermal conductivity of MoS_2 is reported as 34.5 $Wm^{-1}K^{-1}$ from the confocal micro-Raman method[24]. However, it is measured as 13.3 $Wm^{-1}K^{-1}$ in vacuum conditions[25]. Similarly, there are experimental and theoretical studies reporting low cross-planar thermal conductivity in WSe_2 [26–28]. On the other hand, the lattice thermal conductivity of single layer WSe_2 at room temperature is estimated as high as 53 $Wm^{-1}K^{-1}$ based on first-principles calculations[29,30]. Clearly, more studies are necessary in order to resolve the diverse results about the thermal properties of TMDs.

All thermal properties are directly or indirectly related to phonon spectrum which could be obtained from density functional theory (DFT) based calculations at zero

temperature. First-principles studies based on Boltzmann transport equation (BTE) deal with perfect crystal lattice neglecting rippling behavior in single layer materials, moreover they mostly consider three phonon processes. Raman methods are one of the most common approach for experimental studies, and it is very sensitive to sample quality and size. Furthermore, mixed modes and Raman forbidden modes restrict the measurement of frequencies of all phonon modes, and obtained lifetimes are rely on the laser absorption. Classical Molecular Dynamics (MD) simulation is a powerful alternative to overcome all of the aforementioned problems, but its performance depends on the accuracy of inter-atomic potential[31]. In previous works, we have developed parameters for Stillinger-Weber (SW) type potential for TMDs[32,33], and it was shown that the obtained thermal properties are in well agreement with first-principles calculations. As it is quantitatively shown in Ref. 34, the exact prediction of MD thermal conductivity is given by Green-Kubo method where thermal transport properties are driven from the fluctuation dissipation theorem[35,36]. However, one drawback of Green-Kubo method is the lack of possibility of investigating the contribution of different phonon modes and evaluation of phonon lifetimes which is very important in compiling the thermal conductivity. On the other hand, phonon lifetimes and mode contributions are accessible utilizing spectral energy density (SED) method which considers all anharmonic effects as well[37]. Although SED method is widely used in studying 2D materials and their heterostructures[38–42], the investigation of TMDs based on SED is limited[33,43]. Furthermore, most of the previous reports are restricted to optical modes at Γ point or along the high symmetry paths. In this work, we present a systematic study of phonon frequencies and lifetimes of TMDs in full Brillouin zone using mode decomposition and SED method. Contribution of different modes to thermal conductivity are obtained utilizing Callaway model within relaxation time approximation (RTA)[44]. Then, in order to assess the accuracy and limitations of all the mentioned approaches, our results are compared with those from literature obtained from first-principles calculations and Green-Kubo methods, and they are in well agreement specially at high temperatures.

II. METHOD

The SW potential[45] used in this study has the following from,

$$E = \sum_i \sum_{j>i} \phi_2(r_{ij}) + \sum_i \sum_{j\neq i} \sum_{k>j} \phi_3(r_{ij}, r_{ik}, \theta_{ijk}), \quad (1)$$

$$\phi_2(r_{ij}) = A_{ij}\left(\frac{B_{ij}}{r_{ij}^4} - 1\right)\exp\left[\frac{\rho_{ij}}{r_{ij} - r_{ij}^{max}}\right], \quad (2)$$

$$\phi_3(r_{ij}, r_{ik}, \theta_{ijk}) = K_{ijk}\exp\left[\frac{\rho_{ij}}{r_{ij} - r_{ij}^{max}} + \frac{\rho_{ik}}{r_{ik} - r_{ik}^{max}}\right](\cos\theta_{ijk} - \cos\theta_{0,ijk})^2, \quad (3)$$

where the two and three body interactions are defined by ϕ_2 and ϕ_3 respectively. The summations in Eq. 1 run over neighbors of atom i within the radius r^{max} and θ_{ijk} is the angle between two bonds of atom i. Sets of the optimized parameters and more details are presented in previous works[32,33]. There are two different approaches for obtaining phonon dispersion curves using MD. The first one is based on Green's function[46,47] and the other method utilizes SED[37]. The first approach is known to be unstable near the Γ point[47,48]. SED is computationally more expensive but considers all anharmonic effects and generates stable results in entire Brillouin zone and widely used for investigating phonon properties of 2D materials. It is shown that mode decomposition is not necessary and it is possible to use any arbitrary orthogonal set instead of normal mode coordinates[49]. However, mode decomposition makes the study much easier specially when the dispersion curves of different modes are to close to each other. Within the frame work of SED the function $\psi(k, j|t)$ is defined as,

$$\psi(q, j|t) = \sum_{\alpha,b}(\sum_n v_\alpha(n, b|t)exp(-iq.r))e_\alpha^\star(b|q, j), \quad (4)$$

where q is the wave vector, α shows each of the cartesian components of velocity of the b'th basis of the n'th lattice unit cell and $e_\alpha^\star(b|q, j)$ is the j'th normal mode of the perfect crystal lattice. It is shown that the frequency and lifetime of each phonon mode can be obtained by fitting a Lorentzian function,

$$\frac{I}{1 + (\frac{\omega-\omega_0}{\lambda})^2}$$

to power spectrum of $\psi(q, j|t)$. Here, ω_0 is the phonon frequency, $\frac{1}{2\lambda}$ gives the phonon lifetime and I is the peak magnitude. Under the relaxation-time approximation, the contribution of each phonon branch to the lattice thermal conductivity in terms phonon lifetimes τ and group velocities $v_g = \frac{\partial\omega}{\partial q}$ is given by,

$$\kappa_j = \frac{1}{V}\sum_q c_{ph}(v_g(q)\cdot\mathbf{e})^2\tau(q), \quad (5)$$

where κ_j denotes the lattice thermal conductivity along the direction j, V is the volume of the system and $\mathbf{e}$ is the unit vector in the direction of the thermal conductivity. The c_{ph} is the phonon specific heat and it is usual classical form is simplyin terms of Boltzmann constant (k_B). In order to consider the quantum correction at low temperatures, we adapted the quantum mechanical form

given below.

$$c_{ph}(\omega) = \frac{(\hbar\omega)^2}{k_B T} \frac{exp(\hbar\omega/k_B T)}{(exp(\hbar\omega/k_B T) - 1)^2}. \quad (6)$$

All MD simulations in this study have been carried out using open source program LAMMPS[50,51]. In all cases a 70×70 (14700 atoms) triclinic computational cell is relaxed for 500 ps in isothermal-isobaric (NPT) ensemble. Then, the simulation cell constructed using lattice parameters obtained from NPT run and the velocities are recorded in micro-canonical (NVE) ensemble run which is lasted for 2^{20} with time step of 0.5 fs. Periodic boundary conditions are considered in all three dimensions. In order to obtain the averaged power spectrum, 16 different simulations are performed. The Brillouin zone is sampled using 35×35 mesh which is dense enough for the convergence of the summation in equation 5.

III. RESULTS AND DISCUSSIONS

First, we examined the temperature dependent phonon frequencies through the entire Brillouin zone for all the considered materials, WS_2, WSe_2, MoS_2 and $MoSe_2$ by using phonon mode decomposition. Previously, Feng *et al.*[49] have studied the effect of temperature on phonon modes of PbTe and shown that at very high temperatures the harmonic phonon modes are not adequate for decomposing the power spectrum. Although the modes of perfect lattice is used for decomposition in this study, within the considered temperature ranges, up to 500 K the eigenvectors of these modes are quiet accurate to decompose the full power spectrum as demonstrated in the example of performance of phonon mode decomposition shown in Fig S1 of the Supplemental Material[52].

The calculated phonon dispersion curves along the high symmetry directions for five different temperatures (100 - 500 K) are shown in Fig. 1. The results, in particular for acoustic frequencies, are in very good agreement with the ones previously predicted by first-principles approaches. As clearly seen in the figure, the acoustic frequencies do not change notably with temperature compared to the optical frequencies. The most prominent temperature effect is observed on the optical modes of $MoSe_2$, which exhibits considerable red shift by increasing temperature. The evident difference indicates much stronger phonon anharmonicity in this material than the other considered TMDs.

Following the SED calculations, we determined the phonon mode lifetimes, τ, along with the mode frequencies. In Figure 2 the calculated room temperature τ of acoustic modes and an optical mode which has the most contribution in thermal conductivity are presented within the entire first Brillouin zone. The same representation for the other considered temperature values are given in the Supplementary Material[52] as well. The calculated τ values corresponding to the acoustic branches are approximately an order of magnitude longer that the

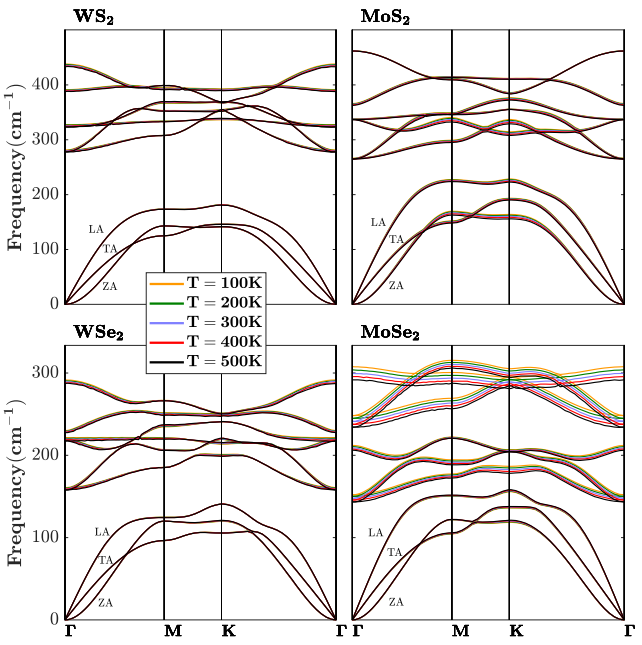

FIG. 1. Phonon dispersion curves of 2D WS_2, WSe_2, MoS_2 and $MoSe_2$ structures calculated by SED approach at different temperatures.

ones calculated for optical modes. For acoustic branches of all the considers materials, the calculated τ values at the phonon wave vectors, q, close to zone center are notably higher. The variation of τ from zone center to zone boundary is very broad and sharp for Mo based systems, whereas this variation is very narrow for W based systems. This characteristic is more evident for the ZA mode. Also, the τ values for W based systems are clearly higher than the ones calculated for Mo based systems. The unusual comparable κ values of heavier W and lighter Mo based layers, previously predicted and also obtained in this study might be related with this notable difference. As anharmonicity is increased from WS_2, WSe_2, MoS_2 to $MoSe_2$, depicted from the frequency shifts in phonon dispersion in Fig. 1, phonon lifetimes are decreased, consequently. The distribution of lifetimes at different q points vary with temperature and the overall trend in lifetimes is only decreasing the mean value by increasing the temperature.

As depicted in the Eq. 5, the another important physical property which has significant contribution on lattice thermal properties is phonon group velocity, v_g. Here, the mode and wave vector decomposed v_g of all the considered materials are calculated by finite difference derivative of phonon frequencies obtained with SED approach within the entire Brillouin zone. In Figure 3, the magnitude of calculated group velocities at room temperature are displayed as similar form with the lifetimes presented above, where v_g data for various other temperatures are reported in the Supplementary Material[52] as well. While τ spectrum characteristics dominated by the

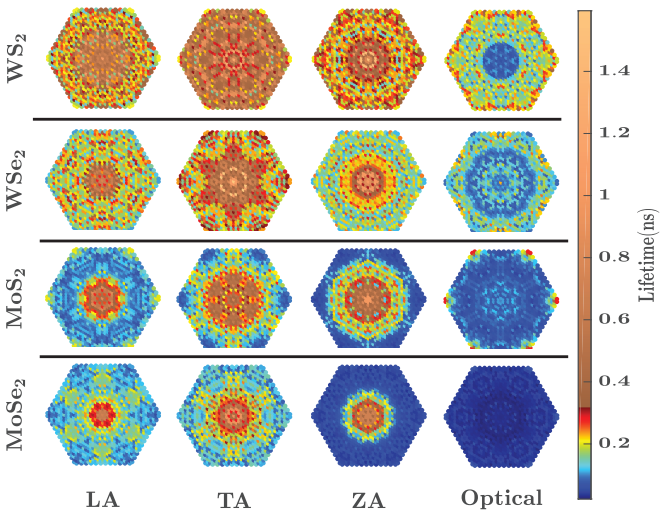

FIG. 2. The calculated Phonon lifetimes by SED approach at 300 K. The represented optical mode is the optical phonon branch which has more contribution in thermal conductivity.

transition metal atoms, here v_g spectrum is dictated by chalcogen atoms, S and Se. This can be explained by the fact that total ionic mass in the unit cell is one of the primary factor for the maximum frequency of acoustic modes, so the Debye temperatures. Among the acoustic modes, ZA branch has quadratic dispersion, feature of 2D systems, that can be observed from circularly symmetric increasing v_g around zone center, Γ point.

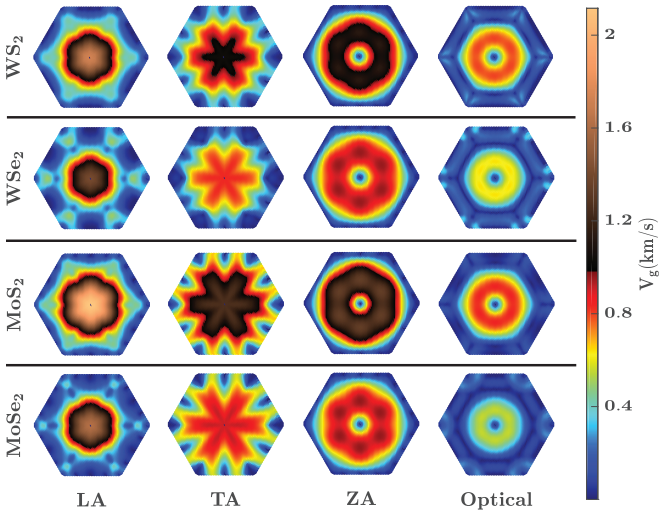

FIG. 3. The magnitude of calculated group velocities at 300 K. The represented optical mode is the optical phonon branch which has more contribution in thermal conductivity.

Eventually, by using Eq. 5 we have investigated lattice thermal conductivity of these materials from the accurately calculated phonon frequency, lifetime and group velocity spectrums which is obtained by SED method achieving highly improved statistical convergence. This approach enables us mode decomposition at any general q point, therefore we can determine contribution of each mode to total lattice thermal conductivity as opposed to other approaches such as Green-Kubo formula. In Fig. 4 the contribution of each mode in thermal conductivity at room temperature is presented. As expected, most of the contribution is from the acoustical modes, however there is a non-negligible contribution from optical modes in WS_2, WSe_2, and MoS_2. On the contrary, the contribution of optical modes of $MoSe_2$ is almost negligible, which is in contrast to the calculated finite v_g values, similar both in WSe_2 and $MoSe_2$. This contrast can be explained by highly anharmonic nature of $MoSe_2$ observed in both as highly suppressed optical phonon lifetimes as seen in Fig.2, and shift in optical frequencies by temperature as seen in Fig.1. Not only optical modes but also relatively low contribution of ZA mode compared to the other acoustical modes and other materials might be another evidence for anharmonicity.

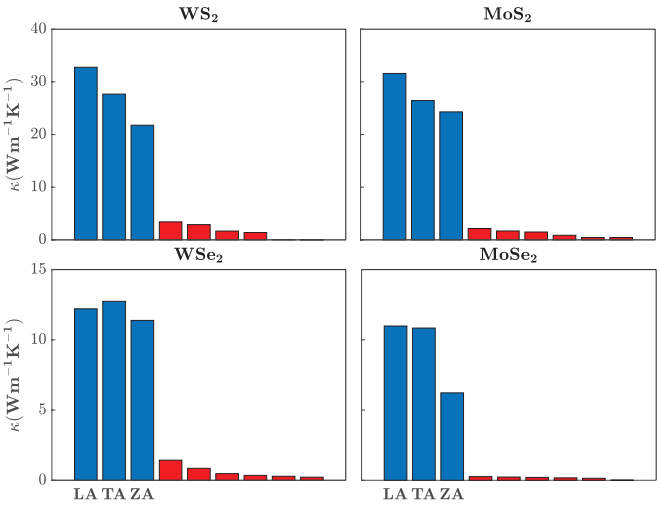

FIG. 4. Contribution of different modes to the room temperature lattice thermal conductivity, the contribution of optical modes are shown by the red bars.

Despite the influence of lifetimes as discussed above, the similar thermal conductivity contributions calculated for acoustic modes of materials with the same chalcogen atom clearly represent the dominant effect of group velocities on final κ values. Therefore, one can conclude that the lattice thermal conductivity scales with total ionic mass in the unit cell for these 2D materials due to the trivial relation between the v_g and ionic mass in any system possessing the same crystal structure.

The contribution of acoustic modes to the lattice thermal conductivity as a function of temperature is shown in Fig. 5. Most of the contribution comes from the LA and TA branches, while ZA mode contribution is less especially in $MoSe_2$ due to the anharmonicity as we discussed above. Overall, in all considered systems, κ decreases with increasing temperature, approximately proportional with inverse temperature as similar to the other

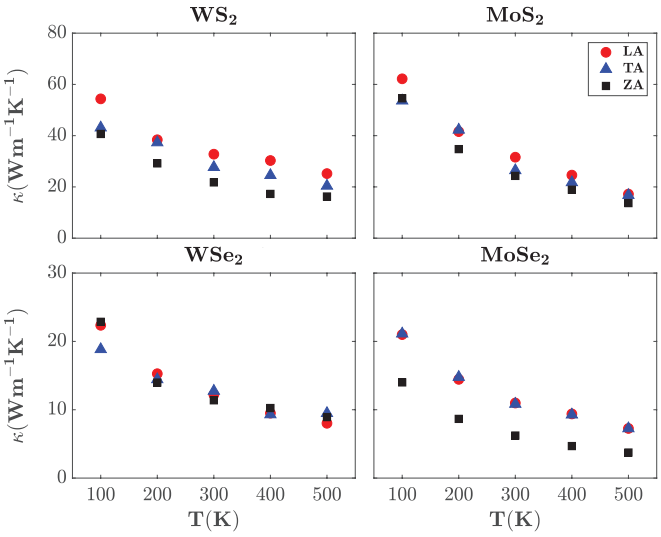

FIG. 5. Temperature dependence of the contribution of acoustic modes to the lattice thermal conductivity.

2D systems[53].

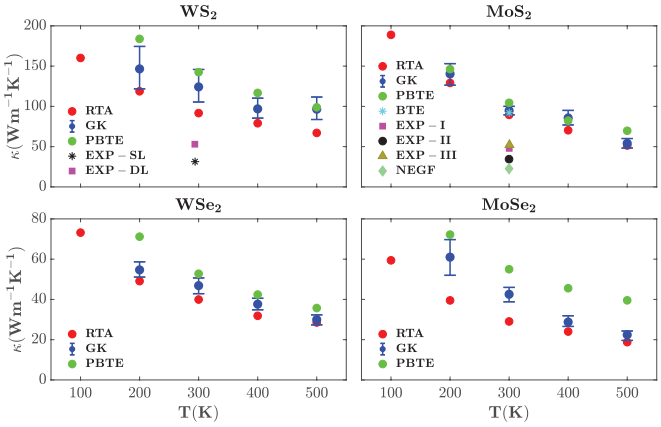

FIG. 6. The lattice thermal conductivity values as a function of temperature. Here, solid red circles are the values calculated in this study, and the values represented by GK, PBTE, BTE, NEGF, EXP-SL, EXP-DL, EXP-I, EXP-II, EXP-III are extracted from (32 and 33), (29), (54), (55), (56), (56), (57), (24), and (58), respectively.

Finally, we predicted the temperature dependent total lattice thermal conductivity values from SED analysis based on MD simulations. The calculated room temperature values, 91.66, 89.43, 39.94, and 29.05 $Wm^{-1}K^{-1}$ for WS_2, MoS_2, WSe_2, and $MoSe_2$ respectively, clearly indicates again the dominant role of chalcogen atom (total ionic mass of the cell) on the overall thermal conductivity. The variation of κ as a function of temperature is depicted in Figure 6 along with the values from the other available methods[29,54]. The total lattice thermal conductivity varies linearly with inverse temperature as predicted for mode decomposed values before. There is an overall agrement between the results of different methods as clearly seen in the figure. The SED method adopted in this study, slightly underestimates, but within the error bars, the κ compared with the Green-Kubo results, which is probably due to the Callaway approach based equation used here[59]. It is possible to include a correction in terms of lifetimes of normal and umklapp processes which cannot be separated from SED analysis. Moreover, the κ values obtained by both MD based approaches are systematically smaller than the first-principles solution of the Phonon Boltzmann Transport Equation, PBTE. This is due to the well known fact that the Maxwell-Boltzmann distributed phonon excitations in the classical molecular dynamics simulations, which enhances the anharmonic interactions, unlike the Fermi-Dirac distributed excitations of phonon modes in PBTE calculations.

IV. CONCLUSIONS

The systematic investigation conducted in this work show that the SED approach used together with classical molecular dynamics calculations is very convenient to study the temperature dependent phonon properties and lattice thermal conductivity. Utilizing multi composition facilitates carrying out a detailed analysis based on mode decomposed lifetimes, group velocities and lattice thermal conductivity, which paves the way to tailor κ of these materials. Thus, with this approach one can also fairly estimate the thermal effects of extended systems like defect and hetero-structure constituted in large super-cell systems, which is not available with methods based on Green-Kubo and first-principles approaches. The most prominent temperature effect is observed on the optical modes of $MoSe_2$, which exhibits considerable red shift by increasing temperature. The evident difference indicates much stronger phonon anharmonicity in this material than the other considered TMDs. On this binary systems, transition metal atoms drive the phonon lifetime values, whereas chalcogen atoms dictates the group velocity spectrum. Most of the contribution to the κ arise from the LA and TA acoustic branches, while ZA mode contribution is less in particular in $MoSe_2$ due to the anharmonicity and quadratic dispersion around Brillouin zone center. In conclusion, for all the considered 2D crystals, κ is linearly proportional with inverse temperature.

V. ACKNOWLEDGMENTS

This work is supported, in part, by The Scientific and Technological Research Council of Turkey (TUBITAK) under the contract number COST-116F445. Computational resources were provided by the High Performance and Grid Computing Center (TRGrid e-Infrastructure) of TUBITAK ULAKBIM, and the National Center for High Performance Computing (UHeM) of Istanbul Technical University; also, in part, by the Center for

Nanoscale Materials, a U.S. Department of Energy Office of Science User Facility, and supported by the U.S. Department of Energy, Office of Science, under Contract No. DE-AC02-06CH11357. CS acknowledges the support from the BAGEP Award of the Science Academy.

[1] D. Jariwala, V. K. Sangwan, L. J. Lauhon, T. J. Marks, and M. C. Hersam, ACS Nano **8**, 1102 (2014).

[2] J. N. Coleman, M. Lotya, A. O'Neill, S. D. Bergin, P. J. King, U. Khan, K. Young, A. Gaucher, S. De, R. J. Smith, I. V. Shvets, S. K. Arora, G. Stanton, H.-Y. Kim, K. Lee, G. T. Kim, G. S. Duesberg, T. Hallam, J. J. Boland, J. J. Wang, J. F. Donegan, J. C. Grunlan, G. Moriarty, A. Shmeliov, R. J. Nicholls, J. M. Perkins, E. M. Grieveson, K. Theuwissen, D. W. McComb, P. D. Nellist, and V. Nicolosi, Science **331**, 568 (2011).

[3] S. Tongay, D. S. Narang, J. Kang, W. Fan, C. Ko, A. V. Luce, K. X. Wang, J. Suh, K. D. Patel, V. M. Pathak, J. Li, and J. Wu, Applied Physics Letters **104**, 012101 (2014).

[4] J. Kang, J. Li, S.-S. Li, J.-B. Xia, and L.-W. Wang, Nano Letters **13**, 5485 (2013).

[5] A. Splendiani, L. Sun, Y. Zhang, T. Li, J. Kim, C.-Y. Chim, G. Galli, and F. Wang, Nano Letters **10**, 1271 (2010).

[6] M. Dendzik, A. Bruix, M. Michiardi, A. S. Ngankeu, M. Bianchi, J. A. Miwa, B. Hammer, P. Hofmann, and C. E. Sanders, Phys. Rev. B **96**, 235440 (2017).

[7] M. Chhowalla, H. S. Shin, G. Eda, L.-J. Li, K. P. Loh, and H. Zhang, Nat Chem **5**, 263 (2013).

[8] Z. Y. Zhu, Y. C. Cheng, and U. Schwingenschlögl, Phys. Rev. B **84**, 153402 (2011).

[9] B. Radisavljevic, A. Radenovic, J. Brivio, V. Giacometti, and A. Kis, Nature Nanotechnology **6**, 147 EP (2011).

[10] W. Liu, J. Kang, D. Sarkar, Y. Khatami, D. Jena, and K. Banerjee, Nano Letters **13**, 1983 (2013).

[11] A. Dankert, L. Langouche, M. V. Kamalakar, and S. P. Dash, ACS Nano **8**, 476 (2014).

[12] H. R. Gutiérrez, N. Perea-López, A. L. Elías, A. Berkdemir, B. Wang, R. Lv, F. López-Urías, V. H. Crespi, H. Terrones, and M. Terrones, Nano Letters **13**, 3447 (2013).

[13] Z. Ye, T. Cao, K. O'Brien, H. Zhu, X. Yin, Y. Wang, S. G. Louie, and X. Zhang, Nature **513**, 214 EP (2014).

[14] K. F. Mak and J. Shan, Nature Photonics **10**, 216 EP (2016), review Article.

[15] C. Lee, J. Hong, M.-H. Whangbo, and J. H. Shim, Chemistry of Materials **25**, 3745 (2013).

[16] W. Huang, X. Luo, C. K. Gan, S. Y. Quek, and G. Liang, Phys. Chem. Chem. Phys. **16**, 10866 (2014).

[17] D. D. Fan, H. J. Liu, L. Cheng, P. H. Jiang, J. Shi, and X. F. Tang, Applied Physics Letters **105**, 133113 (2014).

[18] W. Huang, H. Da, and G. Liang, Journal of Applied Physics **113**, 104304 (2013).

[19] S. Kumar and U. Schwingenschlögl, Chemistry of Materials **27**, 1278 (2015).

[20] X. Xu, J. Chen, and B. Li, Journal of Physics: Condensed Matter **28**, 483001 (2016).

[21] B. Peng, H. Zhang, H. Shao, Y. Xu, X. Zhang, and H. Zhu, RSC Adv. **6**, 5767 (2016).

[22] C. Sevik, Phys. Rev. B **89**, 035422 (2014).

[23] B. D. Kong, S. Paul, M. B. Nardelli, and K. W. Kim, Phys. Rev. B **80**, 033406 (2009).

[24] R. Yan, J. R. Simpson, S. Bertolazzi, J. Brivio, M. Watson, X. Wu, A. Kis, T. Luo, A. R. Hight Walker, and H. G. Xing, ACS Nano **8**, 986 (2014).

[25] J. J. Bae, H. Y. Jeong, G. H. Han, J. Kim, H. Kim, M. S. Kim, B. H. Moon, S. C. Lim, and Y. H. Lee, Nanoscale **9**, 2541 (2017).

[26] C. Chiritescu, D. G. Cahill, N. Nguyen, D. Johnson, A. Bodapati, P. Keblinski, and P. Zschack, Science **315**, 351 (2007).

[27] W.-X. Zhou and K.-Q. Chen, Scientific Reports **5**, 15070 (2015).

[28] P. Norouzzadeh and D. J. Singh, Nanotechnology **28**, 075708 (2017).

[29] X. Gu and R. Yang, Applied Physics Letters **105**, 131903 (2014).

[30] K. Yuan, X. Zhang, L. Li, and D. Tang, Phys. Chem. Chem. Phys. , (2019).

[31] K. Xu, A. J. Gabourie, A. Hashemi, Z. Fan, N. Wei, A. B. Farimani, H.-P. Komsa, A. V. Krasheninnikov, E. Pop, and T. Ala-Nissila, Phys. Rev. B **99**, 054303 (2019).

[32] A. Kandemir, H. Yapicioglu, A. Kinaci, T. Çağın, and C. Sevik, Nanotechnology **27**, 055703 (2016).

[33] A. Mobaraki, A. Kandemir, H. Yapicioglu, O. Gülseren, and C. Sevik, Computational Materials Science **144**, 92 (2018).

[34] A. J. H. McGaughey and M. Kaviany, Phys. Rev. B **69**, 094303 (2004).

[35] M. S. Green, The Journal of Chemical Physics **22**, 398 (1954).

[36] R. Kubo, Journal of the Physical Society of Japan **12**, 570 (1957).

[37] J. A. Thomas, J. E. Turney, R. M. Iutzi, C. H. Amon, and A. J. H. McGaughey, Phys. Rev. B **81**, 081411 (2010).

[38] P. Anees, M. C. Valsakumar, and B. K. Panigrahi, 2D Materials **2**, 035014 (2015).

[39] P. Anees, M. C. Valsakumar, and B. K. Panigrahi, Phys. Chem. Chem. Phys. **18**, 2672 (2016).

[40] Z. Wang, T. Feng, and X. Ruan, Journal of Applied Physics **117**, 084317 (2015).

[41] W. Xu, L. Zhu, Y. Cai, G. Zhang, and B. Li, Journal of Applied Physics **117**, 214308 (2015).

[42] C. da Silva, F. Saiz, D. A. Romero, and C. H. Amon, Phys. Rev. B **93**, 125427 (2016).

[43] P. Anees, M. C. Valsakumar, and B. K. Panigrahi, Applied Physics Letters **108**, 101902 (2016).

[44] J. Callaway, Phys. Rev. **113**, 1046 (1959).

[45] F. H. Stillinger and T. A. Weber, Phys. Rev. B **31**, 5262 (1985).

[46] C. Campañá and M. H. Müser, Phys. Rev. B **74**, 075420 (2006).

[47] L. T. Kong, Computer Physics Communications **182**, 2201 (2011).

[48] E. N. Koukaras, G. Kalosakas, C. Galiotis, and K. Papagelis, Scientific Reports **5**, 12923 EP (2015), article.

[49] T. Feng, B. Qiu, and X. Ruan, Journal of Applied Physics **117**, 195102 (2015).
[50] "Lammps, http://lammps.sandia.gov,".
[51] S. Plimpton, Journal of Computational Physics **117**, 1 (1995).
[52] "See supplemental material at [url will be inserted by publisher] for an example of performance of phonon mode decomposition; and the lifetimes and the group velocities at various temperatures; and the lifetimes as a function of energy at different temperatures.".
[53] T. Kocabaş, D. Çakır, O. Gülseren, F. Ay, N. Kosku Perkgöz, and C. Sevik, Nanoscale **10**, 7803 (2018).
[54] W. Li, J. Carrete, and N. Mingo, Applied Physics Letters **103**, 253103 (2013).
[55] Y. Cai, J. Lan, G. Zhang, and Y.-W. Zhang, Phys. Rev. B **89**, 035438 (2014).
[56] N. Peimyoo, J. Shang, W. Yang, Y. Wang, C. Cong, and T. Yu, Nano Research **8**, 1210 (2015).
[57] I. Jo, M. T. Pettes, E. Ou, W. Wu, and L. Shi, Applied Physics Letters **104**, 201902 (2014).
[58] S. Sahoo, A. P. S. Gaur, M. Ahmadi, M. J.-F. Guinel, and R. S. Katiyar, The Journal of Physical Chemistry C **117**, 9042 (2013).
[59] P. B. Allen, Phys. Rev. B **88**, 144302 (2013).